Visual Abstract

# Efficiency of shape memory alloy seismic restrainers for several conditions of bridge joints

Atef Eraky, Alaa M. Sharabash, Mohamed H. El-Feky
*Zagazig University, Department of Structural Engineering, Egypt.*
*atef_eraky@yahoo.com, a_sharabash@yahoo.com*
*mhfeky@zu.edu.eg, https://orcid.org/0000-0002-4820-1093*

**ABSTRACT.** Movement joints are needed in bridges to accommodate longitudinal expansion and contraction. Enough joint width needs to be available to accommodate not only longitudinal expansion but also expected movements of joints during earthquakes. This may result in excessive joint openings. Devices that can dissipate energy have been suggested to reduce joint displacements. Shape memory alloy (SMA) is one of these energy dissipation devices, which is well known for its ability to return to its natural shape after being deformed. Several cases of bridges and different conditions of seismic events are modeled and tested using developed software programs in MATLAB to show the efficiency of using SMA inside bridge joint openings. These models include the case of two adjacent frames with SMA inside them (2–frames), the case of multi–frames with constant hysteretic SMAs between every two of them (N–frames), the case of multi–frames with constant hysteretic SMAs taking the delay of seismic forces between frames into consideration (delay), and the case of variable masses of bridge frames. Also, parametric studies are performed to show the impacts of all parameters of bridge frames and SMA retrofit devices on seismically joint openings. The results show that the superelastic SMA device plays a huge role in controlling bridge opening and enables limiting the joint width of all models during earthquakes with different values reaching 60% in some cases depending on bridge frame properties, ground motion characteristics, and the hysteretic properties of SMA devices.

**KEYWORDS.** Bridges, Expansion joints, Opening, Earthquakes, SMA, Hysteretic.

OPEN ACCESS

**Citation:** Eraky, A., Sharabash, A.M., El-Feky, M.H., Efficiency of shape memory alloy seismic restrainers for several conditions of bridge joints, Frattura ed Integrità Strutturale, 64 (2023) 104-120.

**Received:** 05.12.2022
**Accepted:** 22.01.2023
**Online first:** 25.01.2023
**Published:** 01.04.2023



## INTRODUCTION

Most bridge decks have movement joints to meet the needs of movements caused by thermal contraction and expansion, substructure settlement, concrete creep and shrinkage, and other factors. The bridge engineering community has learned a lot from previous earthquakes that have happened in the last five decades about the

types of bridge damage that may be predicted in the occurrence of moderate to intense ground shaking. Unseating, as shown in Fig. 1, is one of the most typical forms of bridge failure. The intermediate bridge joint opens as a result of the bridge's adjacent frames moving out of phase during an earthquake. The superstructure of the bridge will unseat and may possibly collapse because of a lack of support if the seat width provided at the joint is smaller than the relative joint gap. Many of the bridges that were damaged in the 1971 San Fernando earthquake displayed this form of failure [1]. On the other hand, during seismic events, adjacent bridge segments may come into collision if the separation gap between them is insufficient to allow their relative motions, which is called earthquake–induced structural pounding. During moderate earthquake motions, this phenomenon may result in localized damage at the contact areas or may lead to severe damage to colliding structures, or perhaps their complete collapse during intense seismic excitations [2]. The third problem with bridge joints is the durability of movement joints. The service life of a joint without maintenance is what is meant by durability in this context. Durability is one of the biggest issues facing bridge owners because of the cost of maintenance and/or poor performance during the joint's service life that may be significantly more than the initial cost. For these reasons, a new design philosophy, which aims to minimize the number of moving deck joints in bridges, in addition to the production of new structural materials, created the necessity for the development of bridge joints with increased moving capacity [3]. Bridge joints have been a hot study area for many years as a result of the aforementioned considerations and the significant role that joints play in bridge pavements and decks.

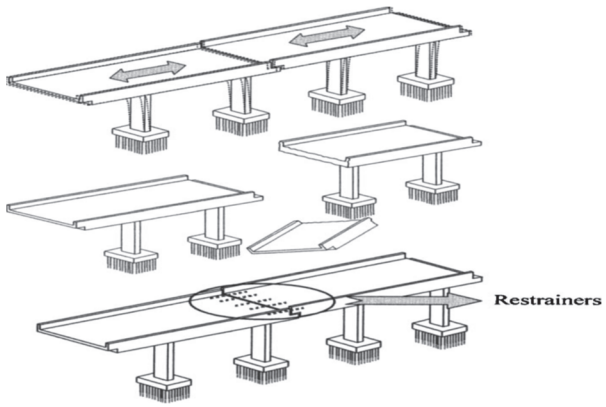


Figure 1: Unseating problems and joint-restrainers placing [1].

To prevent the unseating and pounding of bridge frames and provide durability, researchers have been retrofitting bridge joints using restraining cables. These restraining cables are being placed at the intermediate bridge joints, as shown schematically in Fig. 1, to decrease the relative joint gap and tie the bridge's adjacent frames together in the event of a significant earthquake. There are many types of dampers that play the role of restraining cables. At first, high–strength steel material was used in retrofitting bridges to manufacture restraining cables. After that, other passive control technologies have been suggested for reducing joint displacement, including metallic dampers [4], viscoelastic (VE) solid dampers [5], fluid viscous dampers [6], and others. In this study, another type of damper called shape memory alloy (SMA) is used to control the bridge deck opening. SMA is a type of metallic alloy that has special mechanical characteristics like superelasticity behavior and the shape memory effect. The SMAs' ability to recover their original shape upon unloading is known as their "superelasticity behavior", whereas "shape memory effect" is the deformed alloy's ability to recover its undeformed shape when heated. SMAs are known for their unique thermomechanical characteristics that allow the material to recover its original shape either through heating or removal of stress. These characteristics have encouraged many researchers to study the feasibility of using them in different scientific applications. SMA has been widely used in mechanical, aerospace, and electrical engineering in addition to medical applications. A lot of research has also been done recently on their investigation within civil structural systems [7, 8, 9]. Some experimental advancements are as follows:

- Using SMA as a highway bridge seismic isolation device to limit bearing deformations [10];
- Using SMAs as buildings' and/or cable-stayed bridges' passive energy absorbers helps to reduce displacements and lower system demands [11, 12];
- Installing SMA as fasteners in coastal buildings' walls and roofs to prevent separation during storm occurrences [13];

- When seismic occurrences cause vibrations in the structures, SMA can be used as a tension/compression device in a building's bracing system for advantageous stiffness properties [14];
- Using SMA as a concrete–wire–jacket to enhance concrete confinement [7, 15].

The main goal of this study is to shed some light on the advantages and efficiency of the aforementioned energy dissipation devices (SMAs) for restraining joint–opening in several cases of bridges and different conditions of seismic excitation using verified software programs that were prepared using MATLAB. This study includes four cases: the case of two adjacent frames with one joint opening; the case of multiple frames with multiple joint openings; the case of earthquake impact delay; and the case of variable masses of bridge–frames. Also, a sensitivity study was conducted to show all parameters of bridge–frames and SMAs that affect the ability of SMAs to control relative displacement of bridge–joints.

## METHODOLOGY AND PROGRAMMING

This part has been divided into four sections. In the first section, the equations of motion of two adjacent frames are presented. Secondly, a description of the SMA control device is shown. Thirdly, the bridge model, which was enhanced with the SMA device, and the discussion of the equations of motion of the bridge with SMA are introduced. The last section is the advanced program used for this study.

### *Equation of Motion for Two Adjacent Bridge Frames*

The model used in the numerical study, as shown in Fig. 2a, simulates two bridge–frames as single degree of freedom (SDOF) systems. This model's dynamic equation of motion has the following form [16]:

$$\begin{bmatrix} m_1 & 0 \\ 0 & m_2 \end{bmatrix} \begin{bmatrix} \ddot{x}_1 \\ \ddot{x}_2 \end{bmatrix} + \begin{bmatrix} c_1 & 0 \\ 0 & c_2 \end{bmatrix} \begin{bmatrix} \dot{x}_1 \\ \dot{x}_2 \end{bmatrix} + \begin{bmatrix} k_1 & 0 \\ 0 & k_2 \end{bmatrix} \begin{bmatrix} x_1 \\ x_2 \end{bmatrix} = - \begin{bmatrix} m_1 & 0 \\ 0 & m_2 \end{bmatrix} \begin{bmatrix} 1 \\ 1 \end{bmatrix} \ddot{X}_g \quad (1)$$

where Xi, Ẋi, and Ẍi represent the horizontal displacement, velocity, and acceleration of bridge segment i (i = 1, 2), respectively, while mi, ki, and ci represent the mass, stiffness, and damping coefficients, respectively, and Ẍg represents the acceleration of the input ground motions.

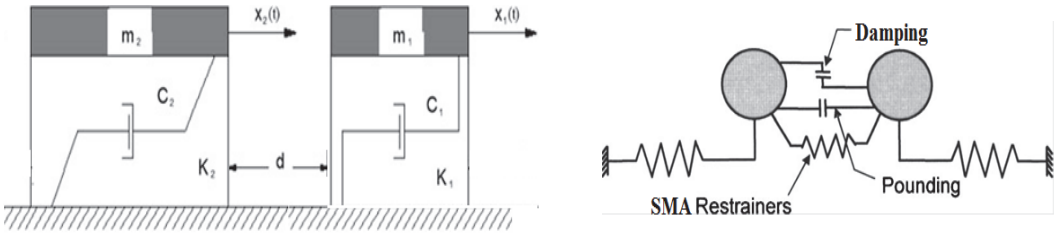


(a) (b)

Figure 2: A bridge with two adjacent frames, (a) Schematic diagram of two adjacent SDOF systems; (b) A Simplified model of 2-DOF bridge.

### *Mechanical Properties of the Shape Memory Alloy*

At ambient temperatures, there are two main phases for shape memory alloys. At low temperatures, SMA is found in its martensite phase, while at high temperatures, it is found in its austenite phase. SMAs experience a phase change when exposed to thermal or mechanical loads. The transition from one phase to the other is accompanied by distinct thermomechanical properties known as "shape memory effect" and "superelasticity". SMA's austenitic phase has a unique superelastic feature that enables the alloy to restore its original shape once the mechanical stress has been eliminated. Fig. 3a shows a schematic for the stress–strain curve of the superelastic SMA. The flat plateau is related to the phase transition to martensite from austenite. As illustrated in Fig. 3a, the elastic strain can reach 8% in some alloys. It is also noticed that

beyond the stage of phase transformation, the alloy experiences strain hardening, which results from the elastic behavior of the martensite. According to previous studies, variations in SMA mechanical characteristics may be linked to a variety of factors, including alloy composition, manufacturing procedure, and strain rate. These factors are important in determining the SMAs' hysterical behavior [17, 18, 19, 20].

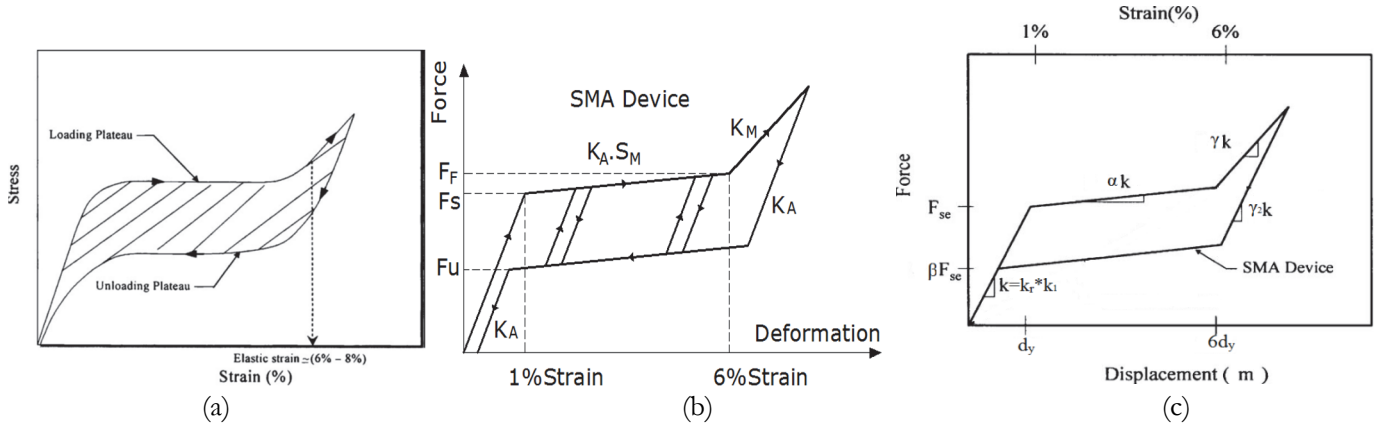


Figure 3: Hysteresis of SMA, (a) A typical stress–strain curve for superelastic SMA [17, 19]; (b) Load–displacement relationship of the chosen superelastic SMA model; (c) Hysteretic parameters of SMA considered in the analysis of this study.

### *Bridge Model*

In this study, a simplified analytical bridge model with two degrees of freedom (2–DOF), which represents a bridge with two adjacent frames, is developed. Fig. 2b shows the model's schematic, which is used for this study. As shown in Fig. 2b, the two adjacent frames are modeled as stick-mass elements. Also, the dashpot is positioned in the system to simulate the equivalent viscous damping in the bridge. The compression/tension link element is suggested to represent the SMA restrainer in the chosen system. The dynamic response of this SMA bridge simulation is guided by the equation below:

$$\begin{bmatrix} m_1 & 0 \\ 0 & m_2 \end{bmatrix}\begin{bmatrix} \ddot{x}_1 \\ \ddot{x}_2 \end{bmatrix}+\begin{bmatrix} c_1 & 0 \\ 0 & c_2 \end{bmatrix}\begin{bmatrix} \dot{x}_1 \\ \dot{x}_2 \end{bmatrix}+\begin{bmatrix} \pm F_{sma} \\ \mp F_{sma} \end{bmatrix}+ \\ \begin{bmatrix} k_1 & 0 \\ 0 & k_2 \end{bmatrix}\begin{bmatrix} x_1 \\ x_2 \end{bmatrix}=-\begin{bmatrix} m_1 & 0 \\ 0 & m_2 \end{bmatrix}\begin{bmatrix} 1 \\ 1 \end{bmatrix}\ddot{x}_g \qquad (2)$$

where Fsma is the restoring force resulting from the SMA restrainer that links the two parts. In Eqns. 1 and 2, some assumptions are made, such as the hinge bearing friction is neglected and there is no gap between bridge segments because SMA fills the joint-opening and carries all colliding forces.

Based on the results of previous studies, it was discovered that the ductility ratio (μ) and the time period ratio (ϱ) had the highest impacts on the bridge hinge openings [17, 18]. The ductility ratio (μ) is the ratio between the maximum displacement and the yield displacement of the frames of the bridge, while the time period ratio (ϱ) is the ratio between the time periods (T) of the two adjacent bridge–frames.

### *Shape Memory Alloy Model*

A simplified one–dimensional tension/compression SMA model is developed and implemented at the bridge's hinge. This model describes the force–displacement relationship of superelastic SMA at a constant temperature, which means that the model is temperature–independent. Fig. 3b presents a schematic of the simplified model's load–displacement relationship for SMA. The parameters primarily used to identify the model's behavior are also shown in Fig. 3b. The parameters include: elastic stiffness at austenite (KA), elastic stiffness at martensite (KM), the load value at the start of phase transformation (FS), the load value at the end of phase transformation (FF) at 6% strain, the ratio of strain hardening at martensitic transformation (SM), and the reverse transformation finishing unloading force (FU). The strain in this model was fixed and set to 1 and 6%, respectively, at the phase transformation start and end.

*Programming*

Many studies have modeled the cyclic loading on several structural elements using different software applications such as ABAQUS finite element code [21, 22, 23], ANSYS finite element code [24, 25, 26, 27, 28], or other control algorithms [29, 30]. In this study, the equations of motion are solved numerically using step–by–step integration of Newmark's method [31], adopting linear variation of acceleration over a small time interval of $\Delta t = 0.001$. MATLAB programs are prepared to perform these tasks. The following flow chart shows the plan of the work of the program, as shown in Fig. 4.

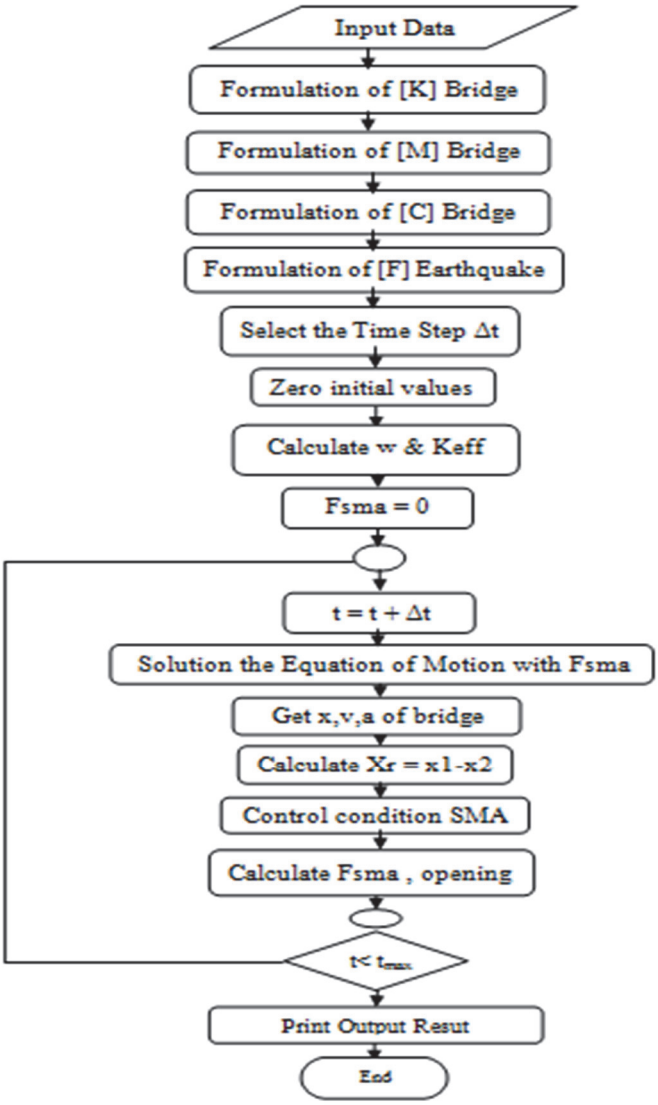


Figure 4: Flow chart of a developed program for a bridge with SMA.

## VALIDATION OF THE NUMERICAL MODEL

A model of two bridge frames is taken in this verification under the results of the WAHO record from the 1989 Loma Prieta earthquake. The record is applied after being scaled to a 0.85 g spectral acceleration at the fundamental period of the structure to accommodate the study performed by Andrawes and DesRoches [17]. Therefore, the response of the opening between two bridge frames is obtained with dynamic characteristics of frames 1 and 2, including constant weight of two frames equal to 22240 kN, the natural time period of the stiffer frame (T1) equals 1.0 sec, and the ductility demand ratio ($\mu$) and period ratio ($\varrho$) of the bridge frames are assumed to be constant and equal to 1.0 and 0.7, respectively. The parameters of the strain hardening ratios of the SMA device are assumed to be constant

and equal to 0.0% and 90% for the transformation stage and martensite stage, respectively. Two types of SMA restrainers with two hysteretic heights are considered in the verification. The β values corresponding to the two types of restrainers are 0.1, which represents a SMA with a thick hysteresis, and 0.9, which represents a SMA with a narrow hysteresis, as shown in Fig. 5.

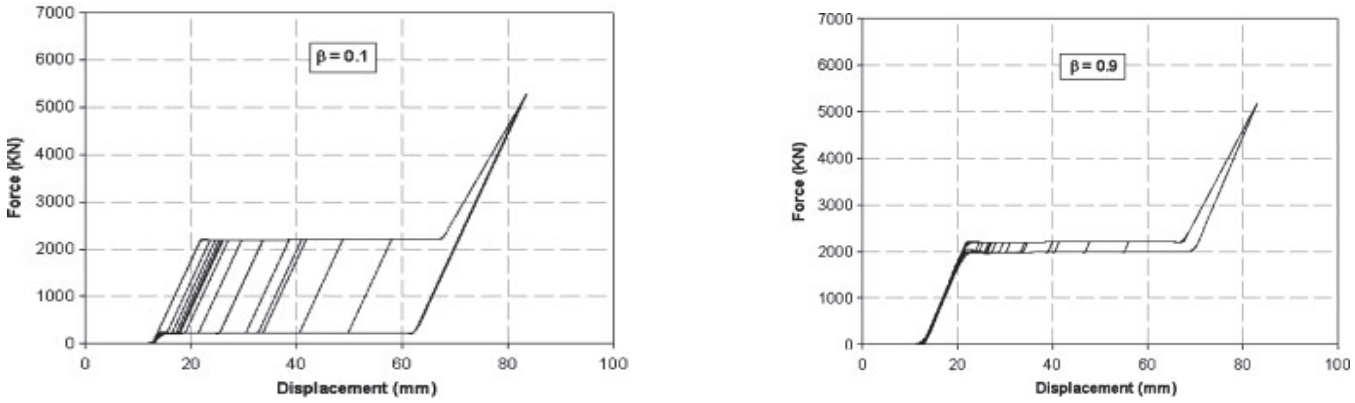


(a) (b)

Figure 5: Load–deformation relationships for the two SMA restrainers with different hysteresis height, (a) Thick hysteresis [17]; (b) Narrow hysteresis [17].

Fig. 6 presents the hinge opening time histories in the case of using the two SMA restrainers in Andrawes study [17] and this study. As displayed in Fig. 6, the maximum hinge opening in both restrainer types is approximately 84 mm for the Andrawes study. On the other hand, the maximum hinge opening in both restrainer types is approximately 81 mm (for β = 0.1) and 85 mm (for β = 0.9) in this study. According to Fig. 6, the numerical results from this study for the maximum hinge opening between two frames with SMA agree roughly with the results from Andrawes [17], with a small difference in the maximum required opening value. It is also shown that there are some differences between the time histories in this study and the Andrawes study because there are some missing data points in the SMA in the Andrawes study that are assumed in the models of this study.

## SENSITIVITY ANALYSIS

It is known that the ideal shape of the SMA hysteresis can lead to the high efficiency of the restrainers in retrofitting hinge openings of bridges and thereby decrease the superstructure pounding/unseating risk throughout seismic events. This task of choosing optimal SMA hysteresis demands a greater understanding of the bridge's sensitivity to the SMA hysteretic properties and shapes. A sensitivity study is conducted using the SMA model that was described previously. For this reason, the effectiveness of SMA in several conditions of bridge joints is presented in the first part. Secondly, the SMA's parameters that most affect the response of the bridge hinge openings are discussed and the effect of interactions between those parameters is examined.

In this study, ten parameters are taken into account, of which four of them are bridge's factors, including period ratio (ϱ) of bridge frames, mass ratio (λ) of bridge frames, natural period of the as-built first bridge frame (T1) that is taken to be equal to 1.0s, and ductility ratio (μ) of bridge frames that is taken to be equal to 1.0 (elastic case) according to previous studies [17]. The other six independent parameters of the SMA hysteretic shape include kr, α, γ, γ2, β, and dy. The six parameters of SMA restrainers are presented in a schematic for the SMA load–deformation curve, as shown in Fig. 3c. The parameter (kr) represents the austenite elastic stiffness that gives the ratio between the austenite elastic stiffness of SMA and the stiffness of the first bridge frame (stiffer segment K1). The parameter (α) represents the ratio of strain hardening at phase transformation. Parameters γ and γ2 represent the ratios of strain hardening during martensitic phase loading and unloading, respectively (γ2 values range from γ value to 1.0). The parameter (β) represents the ratio of the hysteresis height that is defined as the ratio between the load value of the phase transformation start and the load value of the reverse transformation end. The last parameter (dy) represents the deflection at the phase transformation start.

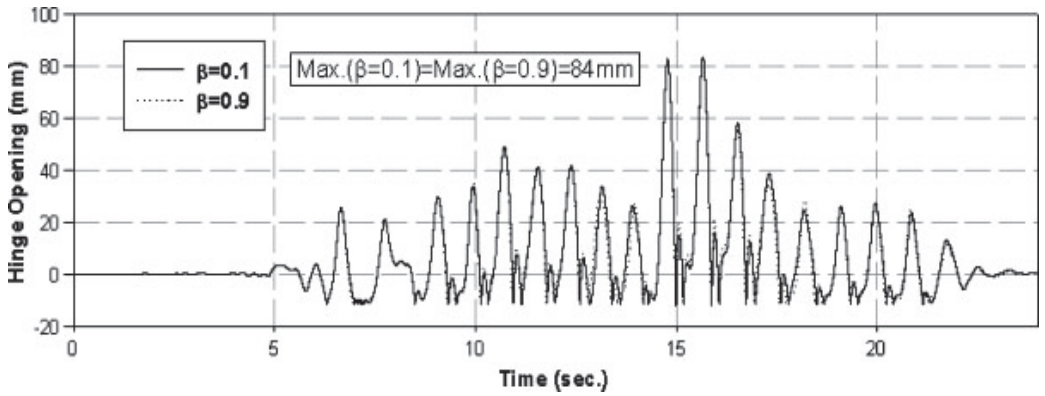


(a)

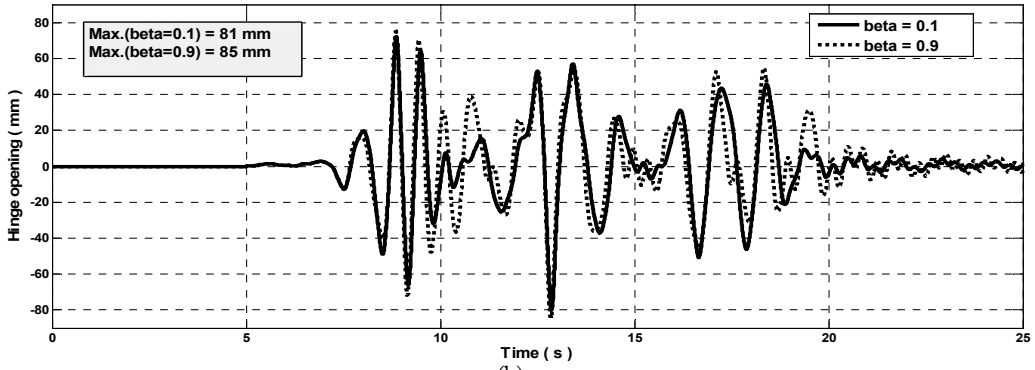


(b)

Figure 6: The time histories of the hinge opening when using SMA hysteresis with thick hysteresis (β=0.1) and narrow hysteresis (β=0.9) under the scaled 1989 Loma Prieta, (a) Andrawes study [17]; (b) Numerical results in this study using MATLAB.

### *Seismic Efficiency of SMA at Bridge Joints*

A comparison between the standard bridge movement joints and the enhanced bridge movement joints using SMA under seismic loads is presented in this study to show how SMA plays a huge role in controlling bridge opening. To simplify this study, some factors are taken as constant values, which are given in Tab. 1 for some cases, including the case of two frames of a bridge with SMA inside them (2–frames); the case of multi frames of a bridge with constant hysteretic SMAs between every two of them (N–frames); the case of multi frames with constant hysteretic SMAs but taking the delay of seismic forces between frames (delay). For the last three cases, the masses of the frames are constant and equal (2224 ton). But in the fourth case, multiple frames of a bridge are taken with constant hysteretic SMAs and variable masses changed by mass ratio (λ). All cases are subjected to Loma Prieta ground motion recordings that are scaled to achieve the target spectral acceleration of 0.8 g at 1.0 s, which is the natural time period of the as–built stiffer bridge segment (T1).

| Parameter | | Case values | | | |
|---|---|---|---|---|---|
| | | Constant mass | | | Variable mass |
| | | 2–frames | N–frames | Delay | |
| Time period T1(s) | | 1.0 | 1.0 | 1.0 | 1.0 |
| Ductility ratio μ | | 1.0 | 1.0 | 1.0 | 1.0 |
| Period ratio ϱ | | [0.3–0.9] | [0.3–0.9] | [0.3–0.9] | [0.3–0.9] |
| Mass ratio λ | | 1.0 | 1.0 | 1.0 | [0.25–1] |
| Damping (Zeta) η | | 0.05 | 0.05 | 0.05 | 0.05 |
| SMA parameters | Kr | 1.67 | 1.67 | 1.67 | 1.67 |
| | α | 0.05 | 0.05 | 0.05 | 0.05 |
| | γ | 0.7 | 0.7 | 0.7 | 0.7 |
| | γ2 | 1.0 | 1.0 | 1.0 | 1.0 |
| | β | 0.4 | 0.4 | 0.4 | 0.4 |
| | dy(m) | 0.007 | 0.007 | 0.007 | 0.007 |

Table 1. Parameter values of the bridge and the SMA used in the study for all cases.

*Case of two–frames of a bridge (2–frames)*

In this case, two adjacent frames from a bridge are taken with equal masses and different stiffness provided by SMA and subjected to the same scaled Loma records. The response of the opening (the difference between the response of two adjacent frames) in the case of without SMA bridge and with SMA bridge is shown in Fig. 7a under the parameters of Tab. 1, where period ratio equals 0.8. Fig. 7a shows that the SMA device has a magic effect on bridge joint width, which reduces the max opening value by about 60% in this condition. Also, Fig. 7b of the load–deformation relationship of the SMA with certain hysteretic parameters, as given in Tab. 1, and a period ratio of 0.8 shows that the energy generated due to this earthquake reduces from 2.5E7 kN.m to 1.8E7 kN.m by about 25% reduction of energy with the help of this SMA damper, which means that the SMA damper is a good energy dissipater.

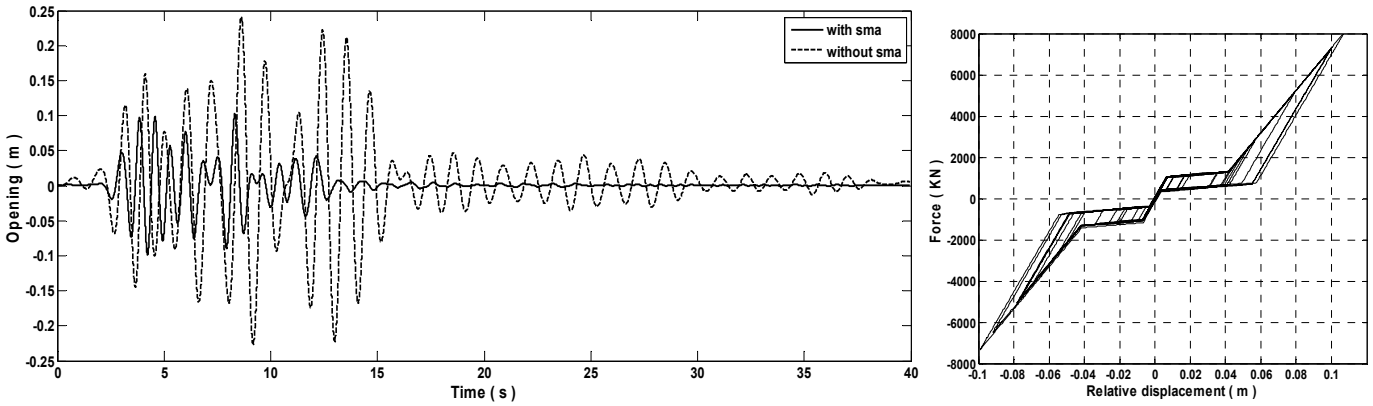


Figure 7: SMA between two adjacent frames of a bridge, (a) Comparing between the time histories of the hinge–opening when using SMA and as–built bridge under the scaled 1989 Loma; (b) Load–deformation relationship of SMA considered in the analysis with period ratio ($\varrho$ = 0.8).

When the time period ratio between the two adjacent bridge frames is changed, the reduction in the maximum response is affected, as shown in Fig. 8. It is shown that the maximum hinge displacement (MHD) of the original structure is affected by the earthquake frequency content, while the bridge provided by SMA has a smaller maximum opening and isn't affected by the earthquake frequency content. It is also shown that MHD (joint opening) tends to decrease as the frame period ratio increases and reaches zero at a period ratio of 1.0 in the two compared cases. As displayed in Fig. 8, the effectiveness of SMA is high in the small values of period ratio compared to period ratio values near to 1.0. At such high period ratios, large relative joint displacements are not predicted to happen since the two adjacent frames act essentially in-phase.

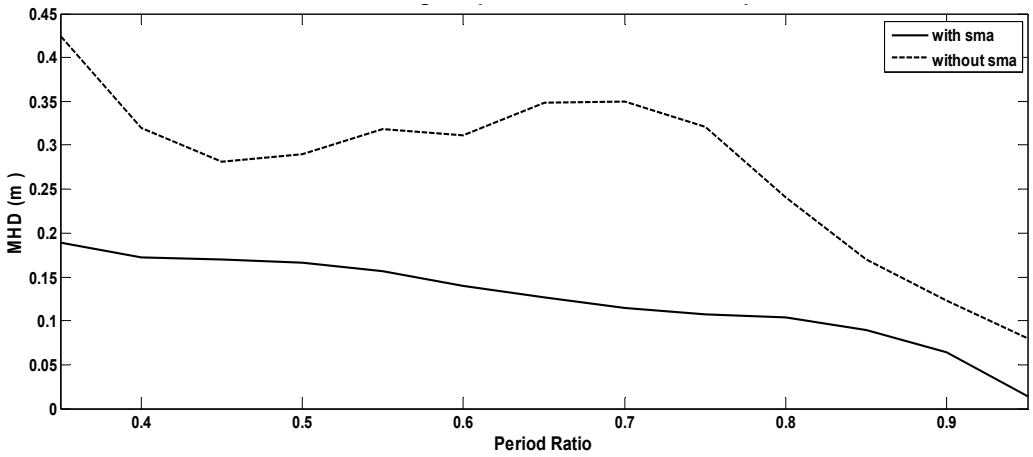


Figure 8: The MHD when using SMA and as–built bridge at various period ratios.

*Case of N–frames of a bridge*

In this case, four adjacent frames from a bridge have been the subject of study with equal mass and different stiffness, which can be calculated from this equation:

$$Ki+1 = \varrho 2 * ki \quad (3)$$

where ki denotes the stiffness coefficient of frame i (i = 1, 2, or 3) in the presence of three SMA among them, using the previous condition but on a multi–frame basis. The essential difference lies in the middle frames where they are exposed to two forces from the SMA on the left and the SMA on the right. The forces that affect every bridge frame can be calculated from these equations:

$$F1 = \Delta F - Fsma1 \quad (4)$$

$$F2 = \Delta F + Fsma1 - Fsma2 \quad (5)$$

$$F3 = \Delta F + Fsma2 - Fsma3 \quad (6)$$

$$F4 = \Delta F + Fsma3 \quad (7)$$

where Fj represents the force of bridge frame j (j = 1, 2, 3, or 4), ΔF and Fsmai denote excitation and retrofit forces from SMA i (i = 1, 2, or 3), respectively. The responses of the three openings (the difference between the responses of every two adjacent frames) in the case of a bridge without SMA and with SMA are shown in Fig. 9 under the parameters in Tab. 1 and a period ratio (ϱ) of 0.8. Fig. 9 shows that the SMA device has a profound effect on bridge joint width, which reduces the max opening value for the three hinges.

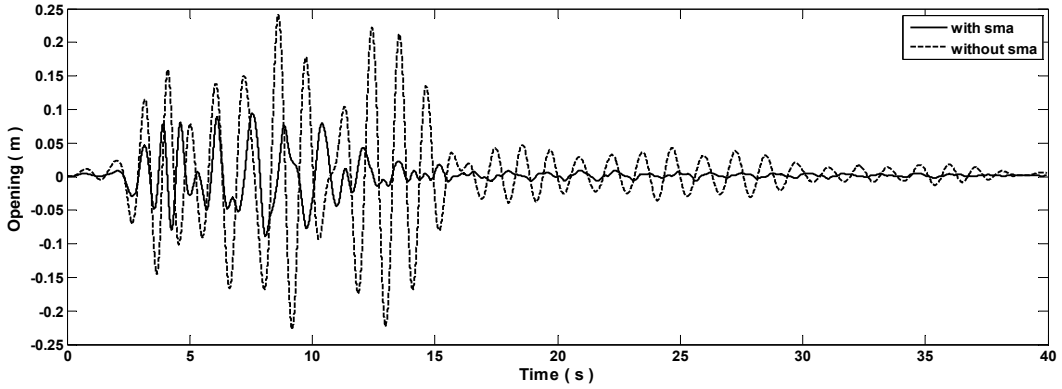


(a)

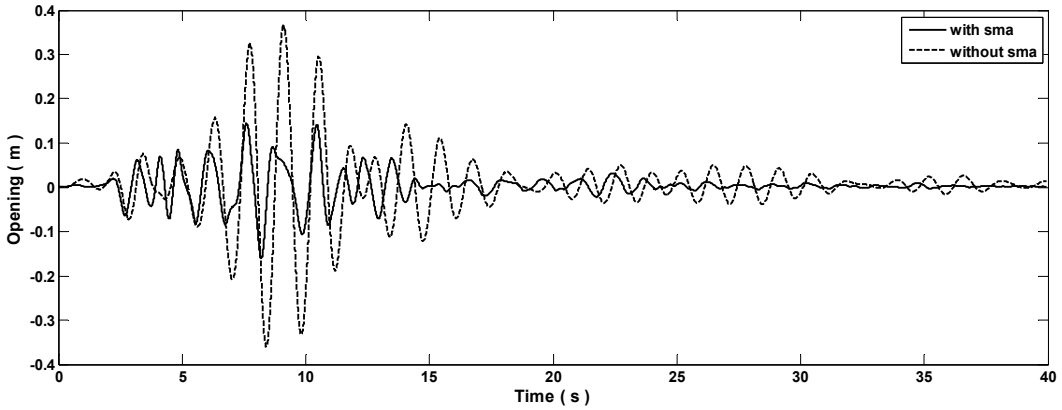


(b)

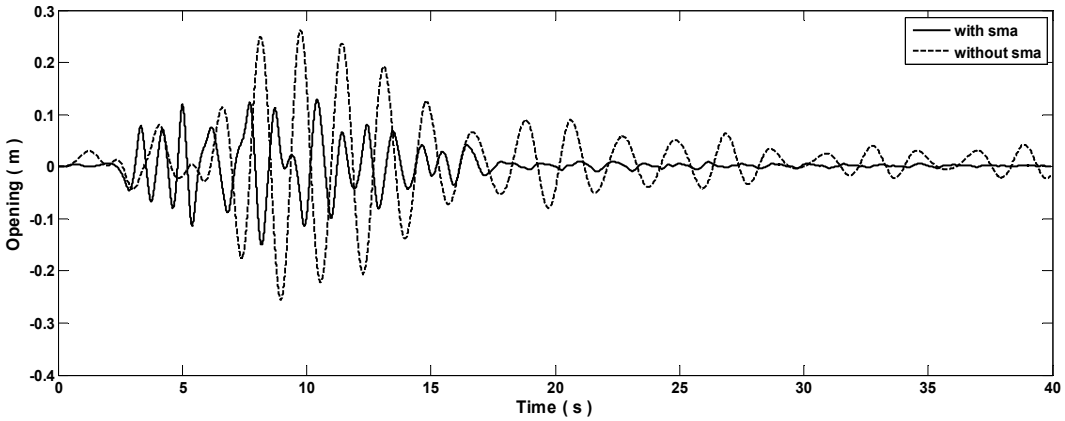


(c)

Figure 9: Comparison between the time histories of three hinges opening when using SMA and as–built bridge under the scaled 1989Loma Prieta record and period ratio (ϱ = 0.8), (a) Hinge 1; (b) Hinge 2; (c) Hinge 3.

Fig. 10 shows MHD with various period ratios for the three openings of this bridge. It is clear from Fig. 10 that opening 3 is the most affected by existing SMA because the stiffness of the last frame of this opening is very small compared to others and, as a result, its frequency (ω) is very small, resulting in a large relative joint displacement, particularly at small (ϱ).

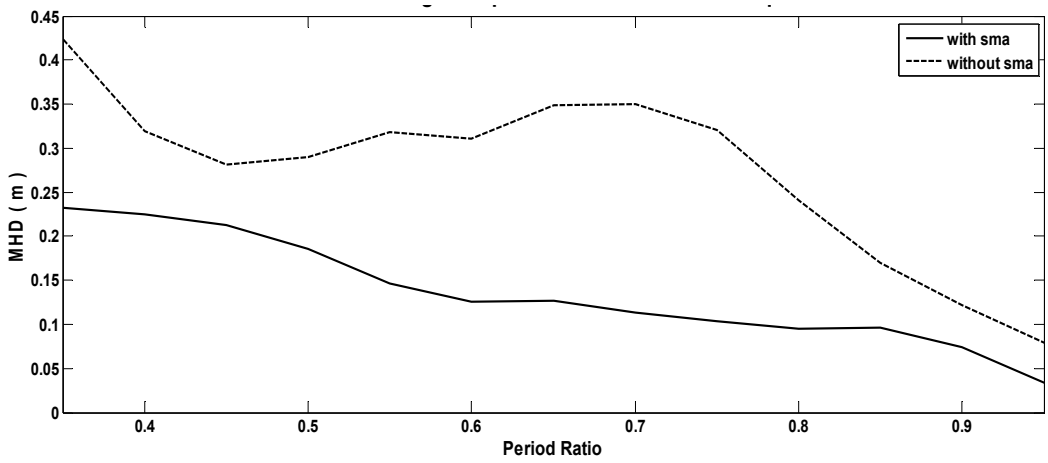


(a)

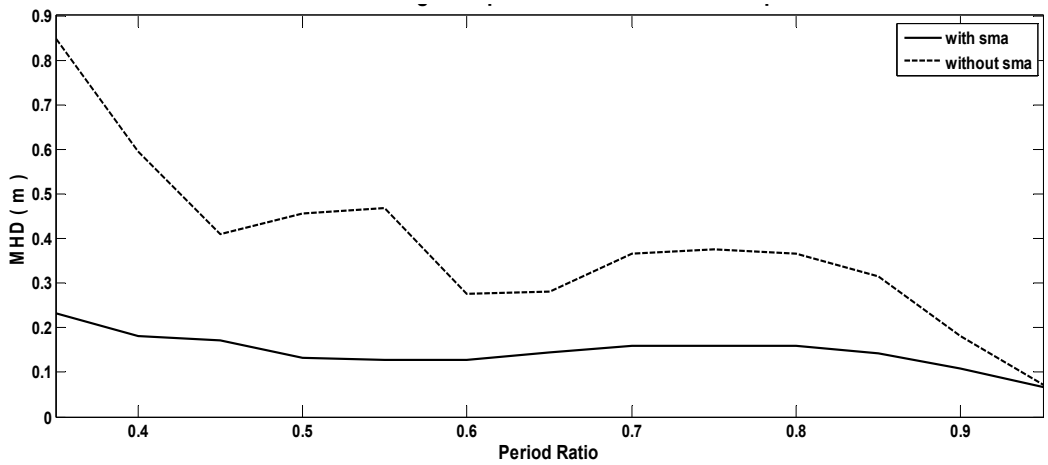


(b)

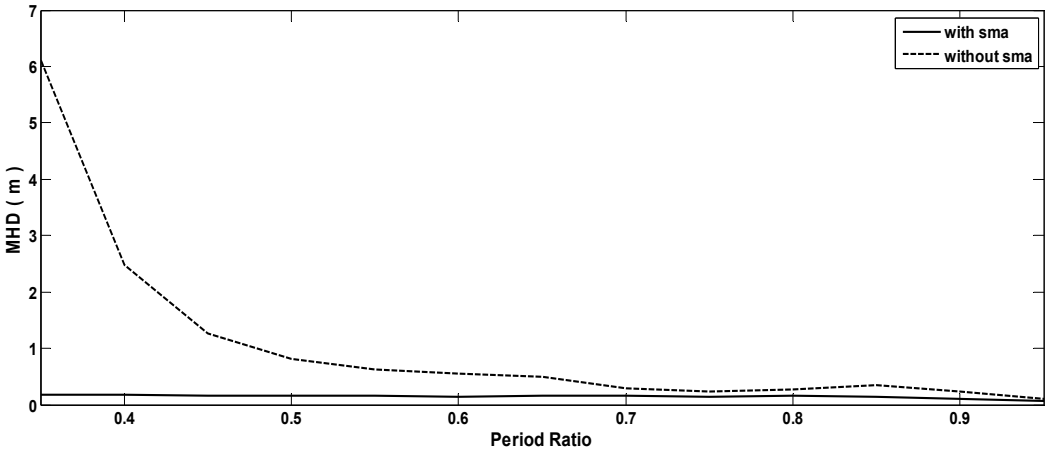


(c)

Figure 10: Comparison between MHD when using SMA and as–built bridge at various period ratios for the three hinges, (a) Hinge 1; (b) Hinge 2; (c) Hinge 3.

*Case of seismic delay*

All the conditions of the N–frames case are met in this case except the ground motion records. The ground motion excitation is explained by identical acceleration recordings shifted in time for various structural bearings along the bridge due to spans between support centers equaling 300m and the velocity of the seismic waves equaling 1000m/s under the Loma earthquake. There is a delay in the earthquake impact, as shown in Fig. 11.

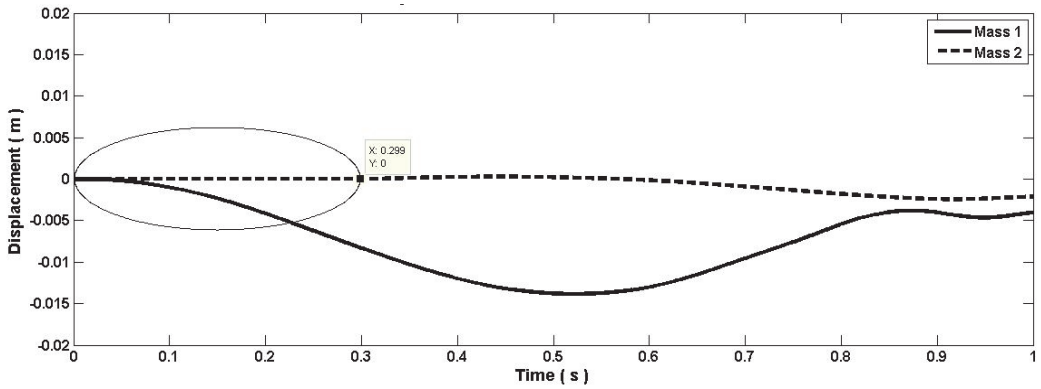


Figure 11: Delay of frame 2 behind frame 1 due to span (300m) and wave's velocity (1000m/s).

As in the N–frames case, the SMA has a pronounced effect on the three hinges' opening, as shown in Fig. 12. It is shown that the SMA dampers effectively reduce the maximum hinge openings in the case of delay. It is also shown that the SMA devices remove the effect of resonance (the high increase in the hinge opening when the frequency of any frame matches the frequency content of the earthquake).

*Case of variable masses of bridge frames*

In the previous cases, the mass ratio λ is taken to be equal to 1.0, meaning that all masses are constant and equal (2224 ton) for the three cases. This case studies the effect of variable masses on SMA's role as a retrofit device, taking the mass of the first frame constant (2224 ton). Fig. 13 shows the variation of the opening with period ratio for four values of mass ratio λ = 1.0, 0.75, 0.5, and 0.25, where mass (m2) and stiffness (k2) of the second frame are calculated from the following equations:

$$m2 = \lambda * m1 \quad (8)$$

$$k2 = \lambda * \varrho 2 * k1 \quad (9)$$

From Fig. 13, it is clear that the efficiency of SMA as a restrainer increases when the mass ratio decreases. This is because when mass ratio decreases, the stiffness of the second frame decreases as well, and so the equivalent stiffness of the second frame with SMA decreases as a result, resulting in a decrease in relative displacement between the two adjacent frames. It is also shown from Fig. 13 that the MHD (opening) values don't change with mass ratios in the case of without SMA because the frequencies of the two frames remain constant. As calculated from Eqns. 8 and 9, the stiffness and mass of the first frame are constants, while those of the second frame are functions of the same variable (λ).

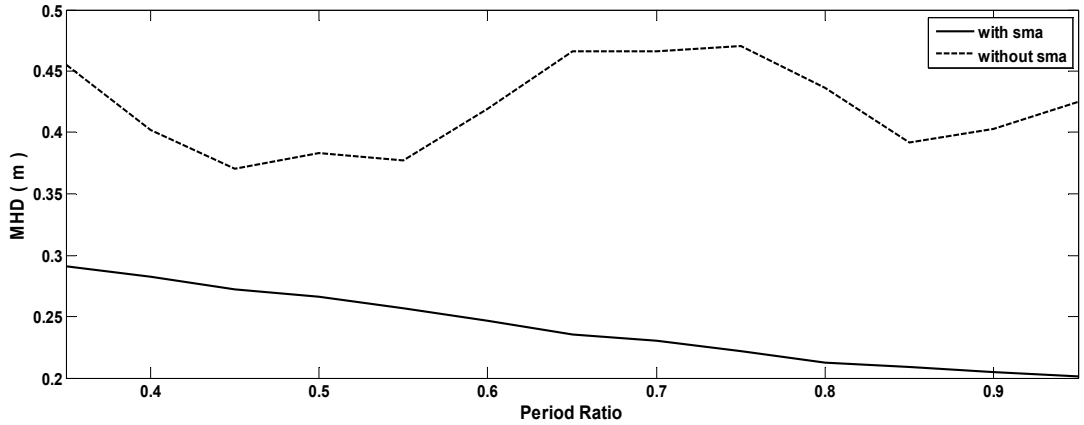


(a)

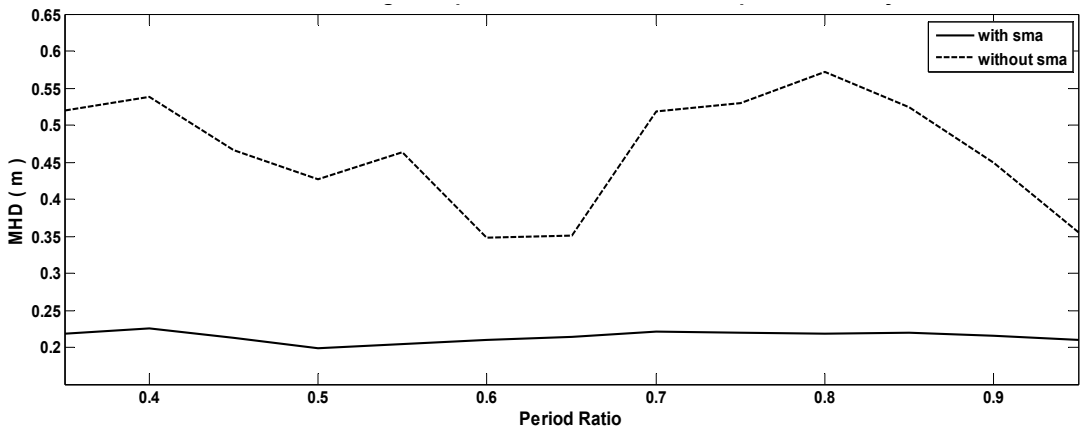


(b)

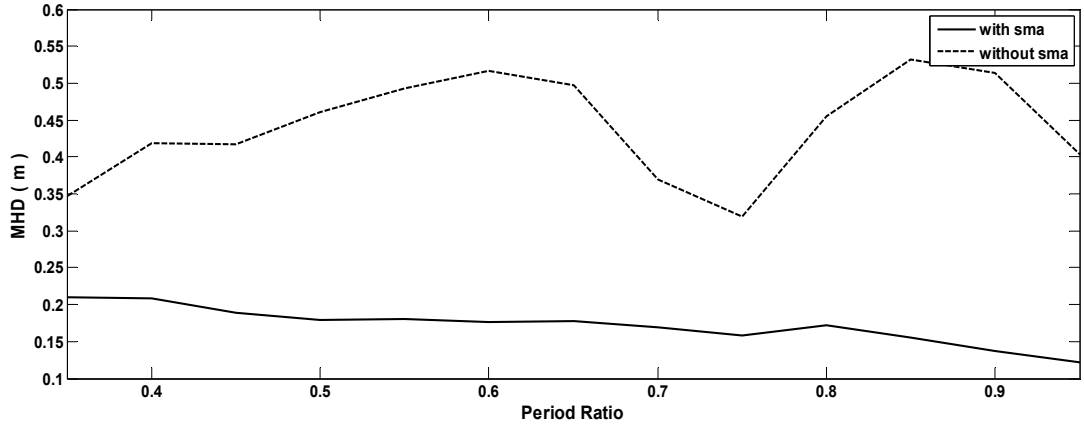


(c)

Figure 12: Comparison between MHD when using SMA and as–built bridge at various period ratios for the three hinges taking delay effect, (a) Hinge 1; (b) Hinge 2; (c) Hinge 3.

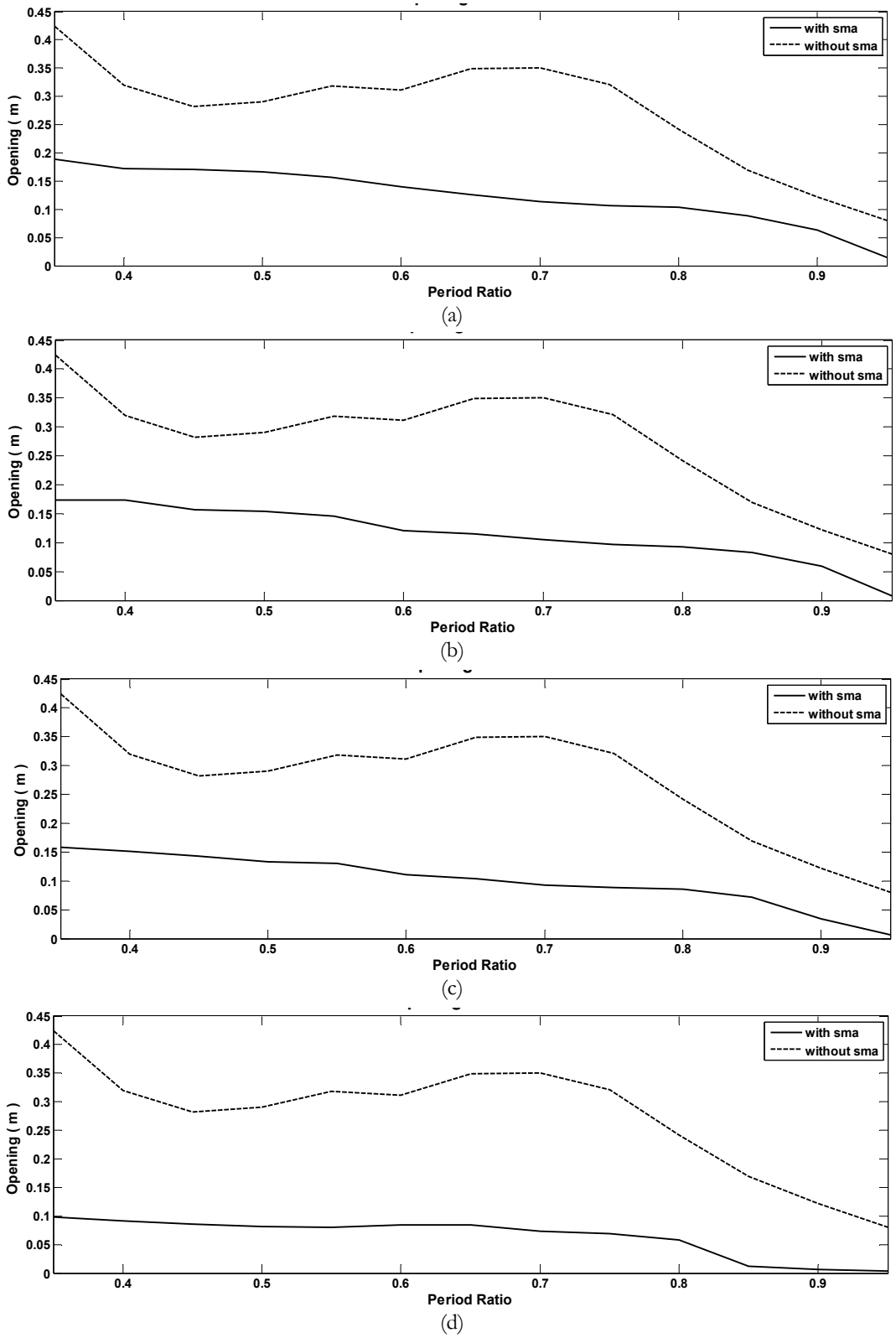


Figure 13: Comparison between MHD (opening) when using SMA and as–built bridge at various period ratios for variable mass ratio λ, (a) Mass ratio λ= 1.0; (b) Mass ratio λ= 0.75; (c) Mass ratio λ= 0.50; (d) Mass ratio λ= 0.25.

### *Effect of SMA Parameters at Bridge Joint width*

SMA parameters are explained earlier in Fig. 3c and Tab. 1. Theoretically, the energy dissipation by SMA plays a big role in SMA's seismic efficiency. Energy dissipation is represented by the area under SMA hysteresis. So, in order to realize the

effect of every parameter, it is required to know what this parameter does in energy dissipation. By taking another look at Fig. 3c and taking energy dissipation into consideration, it can be expected that the effect of all parameters, such as parameters kr, α, γ, and γ2 when increased, energy increased and SMA efficiency increased, but in the opposite, parameters β and dy when decreased, energy increased and SMA efficiency increased.
To confirm this explanation, numerical studies are performed according to values given in Tab. 2 under the scaled Loma earthquake. The first three SMA parameters (kr, α, and γ) are investigated for stiffer frame period values (1.5, 1.0, and 0.6 sec).

| Parameter | | Cases kr effect | α effect | γ effect |
|---|---|---|---|---|
| Mass m1 (ton) | | 2250 | 2250 | 2250 |
| Time period T1(sec) | | (0.6, 1.0, 1.5) | (0.6, 1.0, 1.5) | (0.6, 1.0, 1.5) |
| Ductility ratio μ | | 1.0 | 1.0 | 1.0 |
| Period ratio ϱ | | 0.7 | 0.7 | 0.7 |
| Mass ratio λ | | 0.5 | 0.5 | 0.5 |
| Damping ratio ζ | | 0.05 | 0.05 | 0.05 |
| SMA parameters | kr | [1.0 – 2.0] | 1.67 | 1.67 |
| | α | 0.05 | [0.1 – 1.0] | 0.05 |
| | γ | 0.7 | 0.7 | [0.2 – 1.0] |
| | γ2 | 1.0 | 1.0 | 1.0 |
| | β | 0.4 | 0.4 | 0.4 |
| | dy(m) | 0.007 | 0.0008 | 0.007 |

Table 2: Parameter values of the bridge and the SMA used in the study.

Fig. 14 shows MHD with various austenite stiffness ratios (kr) under constant other parameters, as given in Tab. 2, for the three cases of the stiffer frame period T1 (1.5, 1.0, and 0.6 sec). It is shown that the increase in austenite stiffness ratio (kr) decreases the maximum hinge displacement (MHD) because the higher the austenite stiffness ratio, the higher the resistance of the damper. It is also shown that when the stiffer frame has a time period of 0.6 sec, the MHD has a peak at Kr = 1.5 because the earthquake frequency content is close to the overall system's natural frequency.
Fig. 15 shows MHD with various strains of hardening under constant other parameters, as given in Tab. 2, for the three cases of the stiffer frame period T1 (1.5, 1.0, and 0.6 sec). It is demonstrated that there is no clear relationship during the change in transformation strain hardening values.
Fig. 17 shows MHD with various strains of hardening (γ) under constant other parameters, as given in Tab. 2, for the three cases of the stiffer frame period T1 (1.5, 1.0, and 0.6 sec). It is shown that the increase in strain hardening (γ) decreases the hinge opening due to the increase in dissipated energy.
From Figs. 14, 15, and 16, it can be realised that every parameter has a single effect, compatible with the previous energy dissipation philosophy, without consideration of other factors because other parameters are taken constant during variation of it. But when these conditions change, previous opinion is not applicable, as shown in Figs. 14c and 15a, due to resonance in some cases.

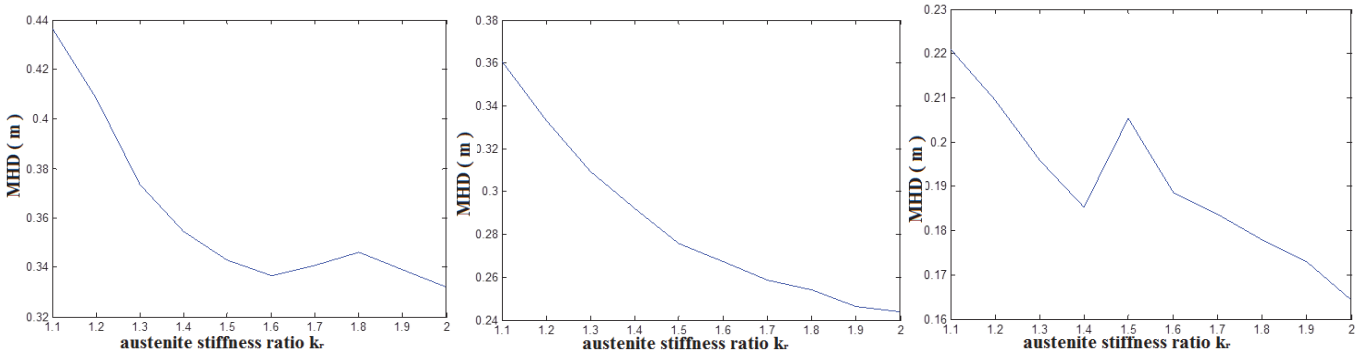


Figure 14: MHD versus variable (kr) values under different periods T1, (a) T1 = 1.5 sec; (b) T1 = 1.0 sec; (c) T1 = 0.6 sec.

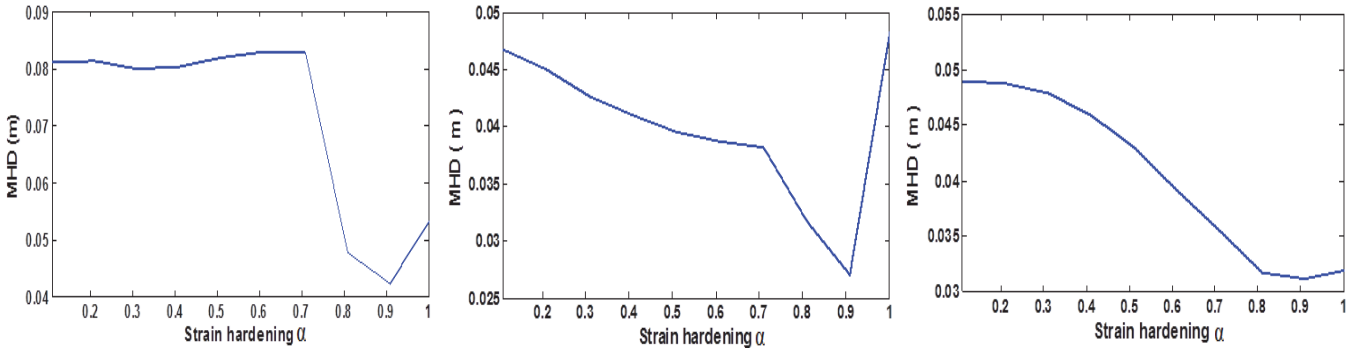


(a) (b) (c)

Figure 15: MHD versus variable (α) values under different periods T1, (a) T1 = 1.5 sec; (b) T1 = 1.0 sec; (c) T1 = 0.6 sec.

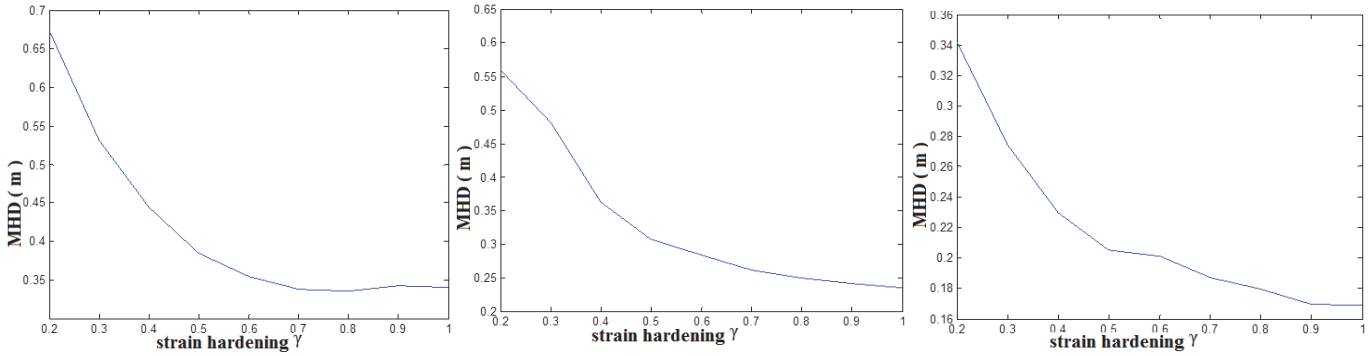


(a) (b) (c)

Figure 16: MHD versus variable (γ) values under different periods T1, (a) T1 = 1.5 sec; (b) T1 = 1.0 sec; (c) T1 = 0.6 sec.

These SMA's parameters depend on variations of other factors, including natural period (T1), seismic records, period ratio (ϱ), mass ratio (λ) and themselves. With the aid of the previously created MATLAP programs of this study, which enable running more models with a wide range of all previous parameters, more trials are required to determine the effectiveness of SMA's parameters on the seismic performance of bridge joints and discover the optimal SMA hysteresis for all types of bridges.

## CONCLUSIONS AND FUTURE RESEARCH

This study analytically explored the enhancement of seismic performance of bridge joints by shape memory alloys with the help of developed MATLAB programs. From the previous analysis of the results, the most important conclusions can be summarized as follows:

- Enhancing bridge joints with SMA dampers enables the limiting of opening width during seismic events by about 60% in some cases of two adjacent bridge frames.
- The SMA dampers can carry the additional forces resulting from the overlap of adjacent hinges in the case of multiple bridge frames under different dynamic loads.
- The SMA dampers reduce the serious effect of resonance when the earthquake frequency is close to the bridge frequency.
- The efficiency of SMA as a restrainer increases when there is a high difference between the two adjacent bay masses.
- The comparison between the standard bridge joint without any dampers and the bridge joint enhanced with SMA dampers in all cases of bridges showed that the addition of SMA dampers improves the joint's ability to accommodate seismic movements, leading to decreased joint width and easier traffic design for the joint under vertical loads.

- Future work will focus on subjecting optimal SMA hysteresis for all types of bridges using previous MATLAB programs to help bridge designers choose suitable SMA restrainers and overcome the two bridge problems of pounding and unseating of bridge decks.

## REFERENCES


[1] Roberts, J.E. (2005). Caltrans structural control for bridges in high-seismic zones. Earthquake engineering & structural dynamics, 34(4-5), pp. 449-470. DOI: 10.1002/eqe.439.

[2] Jankowski, R. and Mahmoud, S. (2015). Earthquake-induced structural pounding. GeoPlanet: Earth and Planetary Sciences, ISBN: 978-3-319-16323-9, Cham: Springer International Publishing Switzerland, pp. 1-156, DOI: 10.1007/978-3-319-16324-6.

[3] Chaallal, O., Sieprawski, G. and Guizani, L. (2006). Fatigue performance of modular expansion joints for bridges. Canadian Journal of Civil Engineering, 33(8), pp. 921-932. DOI: 10.1139/l06-034.

[4] Chen, G., Mu, H. and Both, E.R. (2001). Metallic dampers for seismic design and retrofit of bridges. Rep. No. RDT 01-005, Missouri Dept. of Transportation, Mo. Google Scholar.

[5] Feng, M.Q., Kim, J.M., Shinozuka, M. and Purasinghe, R. (2000). Viscoelastic dampers at expansion joints for seismic protection of bridges. Journal of Bridge Engineering, 5(1), pp. 67-74. DOI: 10.1061/(ASCE)1084-0702(2000)5:1(67).

[6] Moroni, M.O., Boroschek, R. and Sarrazin, M. (2005). Dynamic characteristics of Chilean bridges with seismic protection. Journal of Bridge Engineering, 10(2), pp. 124-132. DOI: 10.1061/(ASCE)1084-0702(2005)10:2(124).

[7] Jung, D., Deogekar, P. and Andrawes, B. (2019). Seismic performance of bridges with high strength concrete columns reinforced with SMA-FRP jackets. Smart Materials and Structures, 28(3), 035008. DOI: 10.1088/1361-665X/aaf6d8.

[8] Zhao, H. and Andrawes, B. (2020). Local strengthening and repair of concrete bridge girders using shape memory alloy precast prestressing plate. Journal of Intelligent Material Systems and Structures, 31(11), pp. 1343-1357. DOI: 10.1177/1045389X20916793.

[9] Sung, M. and Andrawes, B. (2021). Innovative local prestressing system for concrete crossties using shape memory alloys. Engineering Structures, 247, 113048. DOI: 10.1016/j.engstruct.2021.113048.

[10] Wilde, K., Gardoni, P. and Fujino, Y. (2000). Base isolation system with shape memory alloy device for elevated highway bridges. Engineering structures, 22(3), pp. 222-229. DOI: 10.1016/S0141-0296(98)00097-2.

[11] Parulekar, Y.M., Reddy, G.R., Vaze, K.K., Guha, S., Gupta, C., Muthumani, K. and Sreekala, R. (2012). Seismic response attenuation of structures using shape memory alloy dampers. Structural control and health monitoring, 19(1), pp. 102-119. DOI: 10.1002/stc.428.

[12] Sharabash, A.M. and Andrawes, B.O. (2009). Application of shape memory alloy dampers in the seismic control of cable-stayed bridges. Engineering Structures, 31(2), pp. 607-616. DOI: 10.1016/j.engstruct.2008.11.007.

[13] Saadat, S., Noori, M., Davoodi, H., Hou, Z., Suzuki, Y. and Masuda, A. (2001). Using NiTi SMA tendons for vibration control of coastal structures. Smart Materials and Structures, 10(4), 695. DOI: 10.1088/0964-1726/10/4/313.

[14] Speicher, M., Hodgson, D.E., DesRoches, R. and Leon, R.T. (2009). Shape memory alloy tension/compression device for seismic retrofit of buildings. Journal of materials engineering and performance, 18(5), pp. 746-753. DOI: 10.1007/s11665-009-9433-7.

[15] Choi, E., Chung, Y.S., Choi, J.H., Kim, H.T. and Lee, H. (2010). The confining effectiveness of NiTiNb and NiTi SMA wire jackets for concrete. Smart Materials and Structures, 19(3), 035024. DOI: 10.1088/0964-1726/19/3/035024.

[16] Jankowski, R. (2005). Non-linear viscoelastic modeling of earthquake-induced structural pounding. Earthquake engineering & structural dynamics, 34(6), pp. 595-611. DOI: 10.1002/eqe.434.

[17] Andrawes, B. and DesRoches, R. (2007). Effect of hysteretic properties of superelastic shape memory alloys on the seismic performance of structures. Structural Control and Health Monitoring: The Official Journal of the International Association for Structural Control and Monitoring and of the European Association for the Control of Structures, 14(2), pp. 301-320. DOI: 10.1002/stc.159.

[18] Andrawes, B. and DesRoches, R. (2007). Comparison between shape memory alloy seismic restrainers and other bridge retrofit devices. Journal of Bridge Engineering, 12(6), pp. 700-709. DOI: 10.1061/(ASCE)1084-0702(2007)12:6(700).

[19] McCarthy, E., Wright, T., Padgett, J.E., DesRoches, R. and Bradford, P. (2012). Mitigating seismic bridge damage through shape memory alloy enhanced modular bridge expansion joints. Structures Congress, pp. 708-717. DOI: 10.1061/9780784412367.064.
[20] Johnson, R., Padgett, J.E., Maragakis, M.E., DesRoches, R. and Saiidi, M.S. (2008). Large scale testing of nitinol shape memory alloy devices for retrofitting of bridges. Smart materials and structures, 17(3), 035018. DOI: 10.1088/0964-1726/17/3/035018.
[21] Abaqus (2016), Computer Software for Finite Element Analysis, Dassault Systems Simulia; Dassault Systèmes Simulia Corp: Providence, RI, USA.
[22] El-Sisi, A.A., Elgiar, M.M., Maaly, H.M., Shallan, O.A. and Salim, H.A. (2022). Effect of Welding Separation Characteristics on the Cyclic Behavior of Steel Plate Shear Walls. Buildings, 12(7), 879. DOI: 10.3390/buildings12070879.
[23] Shallan, O., Maaly, H., Elgiar, M. and Elsisi, A. (2020). Effect of stiffener characteristics on the seismic behavior and fracture tendency of steel shear walls. Frattura ed Integrità Strutturale, 14(54), pp. 104-115. DOI: 10.3221/IGF-ESIS.54.07.
[24] ANSYS WORKBENCH (2018), Computer Software for Finite Element Analysis, Verification Manual, Release 19.2; ANSYS Inc.: Canonsburg, PA, USA. [Google Scholar]
[25] Sobhy, A., Nour, L.A., Hassan, H. and Elsisi, A. (2021). Behavior of Structural Concrete Frames with Hybrid Reinforcement under Cyclic Loading. Frattura ed Integrità Strutturale, 15(57), pp. 70-81. DOI: 10.3221/IGF-ESIS.57.07.
[26] Amer, A.S., Abdel Kader, H., Abdel-Razek, L. and El-Sisi, A.E.D. (2021). Numerical analysis of FRP reinforced frames under cyclic loading. The Egyptian International Journal of Engineering Sciences and Technology, 34(1), pp. 28-37. DOI: 10.21608/eijest.2021.60164.1045.
[27] Mohamed, G.A., Eisa, A.S., Purcz, P. and El-Feky, M.H. (2021). Theoretical study on the flexural behavior of structural elements strengthened with external pre-stressing methods. Appl. Sci., 12, 171. DOI: 10.3390/app12010171.
[28] Mohamed, G.A., Eisa, A.S., Purcz, P., Ručinský, R. and El-Feky, M.H. (2022). Effect of external tendon profile on improving structural performance of RC beams. Buildings, 12, 789. DOI: 10.3390/buildings12060789.
[29] Nikos, G.P. and Charis, J.G. (2011). Influence of time delay and saturation capacity in control of structures under seismic excitations. Smart Structures and systems, An International Journal, 8(5), pp. 479-490. DOI: 10.12989/sss.2011.8.5.449
[30] Nikos, G.P. (2017). Pole placement algorithm for control of civil structures subjected to earthquake excitation. Journal of Applied and computational mechanics, 3(1), pp. 25-36. DOI: 10.22055/jacm.2017.12603.
[31] Newmark, N. M. (1959). A method of computation for structural dynamics. Journal of the engineering mechanics division, 85(3), pp. 67-94. DOI: 10.1061/JMCEA3.0000098.